Observation of $B^+ \to p\bar{p}\pi^+$, $B^0 \to p\bar{p}K^0$, and $B^+ \to p\bar{p}K^{*+}$

M.-Z. Wang,[23] K. Abe,[7] K. Abe,[40] T. Abe,[7] I. Adachi,[7] H. Aihara,[42] Y. Asano,[47] T. Aso,[46] V. Aulchenko,[1] T. Aushev,[11] A. M. Bakich,[37] A. Bay,[16] I. Bizjak,[12] A. Bondar,[1] A. Bozek,[24] M. Bračko,[18,12] T. E. Browder,[6] M.-C. Chang,[23] P. Chang,[23] Y. Chao,[23] K.-F. Chen,[23] B. G. Cheon,[36] R. Chistov,[11] S.-K. Choi,[5] Y. Choi,[36] Y. K. Choi,[36] P. H. Chu,[23] A. Chuvikov,[31] M. Danilov,[11] L. Y. Dong,[9] A. Drutskoy,[11] S. Eidelman,[1] V. Eiges,[11] C. Fukunaga,[44] N. Gabyshev,[7] A. Garmash,[1,7] T. Gershon,[7] G. Gokhroo,[38] B. Golob,[17,12] T. Hara,[28] H. Hayashii,[21] M. Hazumi,[7] T. Hokuue,[20] Y. Hoshi,[40] W.-S. Hou,[23] H.-C. Huang,[23] K. Inami,[20] A. Ishikawa,[20] R. Itoh,[7] H. Iwasaki,[7] M. Iwasaki,[42] Y. Iwasaki,[7] J. H. Kang,[51] N. Katayama,[7] H. Kawai,[2] T. Kawasaki,[26] H. Kichimi,[7] H. J. Kim,[51] Hyunwoo Kim,[14] J. H. Kim,[36] S. K. Kim,[35] K. Kinoshita,[3] P. Koppenburg,[7] S. Korpar,[18,12] P. Križan,[17,12] P. Krokovny,[1] A. Kuzmin,[1] Y.-J. Kwon,[51] J. S. Lange,[4,32] S. H. Lee,[35] T. Lesiak,[24] A. Limosani,[19] S.-W. Lin,[23] J. MacNaughton,[10] G. Majumder,[38] F. Mandl,[10] T. Matsumoto,[44] W. Mitaroff,[10] H. Miyake,[28] H. Miyata,[26] T. Nagamine,[41] Y. Nagasaka,[8] E. Nakano,[27] S. Nishida,[7] O. Nitoh,[45] S. Ogawa,[39] T. Ohshima,[20] S. Okuno,[13] S. L. Olsen,[6] W. Ostrowicz,[24] H. Ozaki,[7] P. Pakhlov,[11] H. Palka,[24] C.W. Park,[14] H. Park,[15] N. Parslow,[37] L. E. Piilonen,[49] M. Rozanska,[24] H. Sagawa,[7] S. Saitoh,[7] Y. Sakai,[7] T. R. Sarangi,[48] O. Schneider,[16] A. J. Schwartz,[3] S. Semenov,[11] H. Shibuya,[39] V. Sidorov,[1] J. B. Singh,[29] N. Soni,[29] S. Stanič,[47,*] M. Starič,[12] A. Sugiyama,[33] K. Sumisawa,[28] T. Sumiyoshi,[44] S. Suzuki,[50] S. Y. Suzuki,[7] F. Takasaki,[7] K. Tamai,[7] N. Tamura,[26] M. Tanaka,[7] Y. Teramoto,[27] T. Tomura,[42] T. Tsuboyama,[7] T. Tsukamoto,[7] S. Uehara,[7] S. Uno,[7] G. Varner,[6] K. E. Varvell,[37] C. H. Wang,[22] J. G. Wang,[49] Y. Watanabe,[43] Y. Yamada,[7] A. Yamaguchi,[41] Y. Yamashita,[25] M. Yamauchi,[7] H. Yanai,[26] J. Ying,[30] Y. Yuan,[9] Y. Yusa,[41] C. C. Zhang,[9] Z. P. Zhang,[34] V. Zhilich,[1] and D. Žontar[17,12]

(Belle Collaboration)

[1]*Budker Institute of Nuclear Physics, Novosibirsk*
[2]*Chiba University, Chiba*
[3]*University of Cincinnati, Cincinnati, Ohio 45221*
[4]*University of Frankfurt, Frankfurt*
[5]*Gyeongsang National University, Chinju*
[6]*University of Hawaii, Honolulu, Hawaii 96822*
[7]*High Energy Accelerator Research Organization (KEK), Tsukuba*
[8]*Hiroshima Institute of Technology, Hiroshima*
[9]*Institute of High Energy Physics, Chinese Academy of Sciences, Beijing*
[10]*Institute of High Energy Physics, Vienna*
[11]*Institute for Theoretical and Experimental Physics, Moscow*
[12]*J. Stefan Institute, Ljubljana*
[13]*Kanagawa University, Yokohama*
[14]*Korea University, Seoul*
[15]*Kyungpook National University, Taegu*
[16]*Institut de Physique des Hautes Énergies, Université de Lausanne, Lausanne*
[17]*University of Ljubljana, Ljubljana*
[18]*University of Maribor, Maribor*
[19]*University of Melbourne, Victoria*
[20]*Nagoya University, Nagoya*
[21]*Nara Women's University, Nara*
[22]*National Lien-Ho Institute of Technology, Miao Li*
[23]*Department of Physics, National Taiwan University, Taipei*
[24]*H. Niewodniczanski Institute of Nuclear Physics, Krakow*
[25]*Nihon Dental College, Niigata*
[26]*Niigata University, Niigata*
[27]*Osaka City University, Osaka*
[28]*Osaka University, Osaka*
[29]*Panjab University, Chandigarh*
[30]*Peking University, Beijing*
[31]*Princeton University, Princeton, New Jersey 08545*
[32]*RIKEN BNL Research Center, Upton, New York 11973*
[33]*Saga University, Saga*
[34]*University of Science and Technology of China, Hefei*

 0031-9007/04/92(13)/131801(6)$22.50

[35]*Seoul National University, Seoul*
[36]*Sungkyunkwan University, Suwon*
[37]*University of Sydney, Sydney NSW*
[38]*Tata Institute of Fundamental Research, Bombay*
[39]*Toho University, Funabashi*
[40]*Tohoku Gakuin University, Tagajo*
[41]*Tohoku University, Sendai*
[42]*Department of Physics, University of Tokyo, Tokyo*
[43]*Tokyo Institute of Technology, Tokyo*
[44]*Tokyo Metropolitan University, Tokyo*
[45]*Tokyo University of Agriculture and Technology, Tokyo*
[46]*Toyama National College of Maritime Technology, Toyama*
[47]*University of Tsukuba, Tsukuba*
[48]*Utkal University, Bhubaneswer*
[49]*Virginia Polytechnic Institute and State University, Blacksburg, Virginia 24061*
[50]*Yokkaichi University, Yokkaichi*
[51]*Yonsei University, Seoul*
(Received 11 October 2003; published 1 April 2004)

We report the first observation of a $b \to u$ type charmless baryonic B decay, $B^+ \to p\bar{p}\pi^+$, as well as $b \to s$ type $B^0 \to p\bar{p}K^0$ and $B^+ \to p\bar{p}K^{*+}$ decays. The analysis is based on a 78 fb^{-1} data sample recorded on the $\Upsilon(4S)$ resonance with the Belle detector at KEKB. We find $\mathcal{B}(B^+ \to p\bar{p}\pi^+) = (3.06^{+0.73}_{-0.62} \pm 0.37) \times 10^{-6}$, $\mathcal{B}(B^0 \to p\bar{p}K^0) = (1.88^{+0.77}_{-0.60} \pm 0.23) \times 10^{-6}$, and $\mathcal{B}(B^+ \to p\bar{p}K^{*+}) = (10.3^{+3.6+1.3}_{-2.8-1.7}) \times 10^{-6}$. We also update $\mathcal{B}(B^+ \to p\bar{p}K^+) = (5.66^{+0.67}_{-0.57} \pm 0.62) \times 10^{-6}$ and present an upper limit on $\mathcal{B}(B^0 \to p\bar{p}K^{*0})$ at the 90% confidence level. A common feature of the observed decay modes is threshold peaking in baryon pair invariant mass.

DOI: 10.1103/PhysRevLett.92.131801 PACS numbers: 13.25.Hw, 13.60.Rj

The Belle Collaboration recently reported the observation of $B^+ \to p\bar{p}K^+$ [1] and $B^0 \to p\bar{\Lambda}\pi^-$ [2] decays. These are the first examples of B meson decays to charmless three-body final states containing baryons and are candidates for $b \to s$ penguin transitions. Our observation of these modes has stimulated much theoretical interest [3–9] because these decay channels may be used to test our theoretical understanding of rare decay processes involving baryons and search for direct CP violation. One interesting feature of the observation is that the baryon pair mass spectra seem to peak toward threshold as originally conjectured by Refs. [10,11]. Lately more speculations on this have been proposed [7–9]. In this Letter we report the first observation of $B^+ \to p\bar{p}\pi^+$ [12], which is dominated by the $b \to u$ tree diagram. We also report the first observation of $B^0 \to p\bar{p}K^0$ and $B^+ \to p\bar{p}K^{*+}$ decays and improve the measurement of $B^+ \to p\bar{p}K^+$. A search for the $B^0 \to p\bar{p}K^{*0}$ mode yields only an upper limit. With these new results we study the $p\bar{p}$ mass spectra to see if the threshold peaking observed in our previous results is confirmed with the newly observed modes.

We use a 78 fb^{-1} data sample, consisting of $(85.0 \pm 0.5) \times 10^6$ $B\bar{B}$ pairs, collected by the Belle detector at the KEKB asymmetric energy e^+e^- (3.5 on 8 GeV) collider [13]. The Belle detector is a large solid angle magnetic spectrometer that consists of a three layer silicon vertex detector (SVD), a 50 layer central drift chamber (CDC), an array of aerogel threshold Čerenkov counters (ACC), a barrel-like arrangement of time of flight scintillation counters (TOF), and an electromagnetic calorimeter comprised of CsI (Tl) crystals located inside a superconducting solenoid coil that provides a 1.5 T magnetic field. An iron flux return located outside of the coil is instrumented to detect K_L^0 mesons and to identify muons. The detector is described in detail elsewhere [14].

The event selection criteria are based on the information obtained from the tracking system (SVD + CDC) and the hadron identification system (CDC + ACC + TOF) and are optimized using Monte Carlo (MC) simulated event samples. All primary charged tracks are required to satisfy track quality criteria based on the track impact parameters relative to the interaction point (IP). The deviations from the IP position are required to be within ± 1 cm in the transverse (x-y) plane, and within ± 3 cm in the z direction, where the z axis is defined by the positron beam line. Proton, kaon, and pion candidates are selected using $p/K/\pi$ likelihood functions obtained from the hadron identification system. For protons, we require $L_p/(L_p + L_K) > 0.6$ and $L_p/(L_p + L_\pi) > 0.6$, where $L_{p/K/\pi}$ stands for the proton/kaon/pion likelihood. We require $L_K/(L_K + L_\pi) > 0.6$ to identify kaons and $L_\pi/(L_K + L_\pi) > 0.6$ for pions. K_S^0 candidates are reconstructed via the $\pi^+\pi^-$ decay channel and have an invariant mass with $|M_{\pi^+\pi^-} - M_{K^0}| < 30$ MeV/c^2. The candidate must have a displaced vertex and flight direction consistent with a K_S^0 originating from the interaction point. We use the selected kaons and pions to form K^{*+} ($\to K_S^0\pi^+$) and K^{*0} ($\to K^+\pi^-$) candidates by requiring the invariant mass of the combination to be within

80 MeV/c^2 of the K^* mass. The numbers used are 892 and 896 MeV/c^2 for $M_{K^{*+}}$ and $M_{K^{*0}}$, respectively. To ensure the decay process is genuinely charmless, we apply the charm veto. The regions $2.85 < M_{p\bar{p}} < 3.128$ GeV/c^2 and $3.315 < M_{p\bar{p}} < 3.735$ GeV/c^2 are excluded to remove background from modes with η_c, J/ψ and ψ', χ_{c0}, χ_{c1} mesons, respectively. The region $2.262 < M_{pK_S^0} < 2.310$ GeV/c^2 is excluded to remove Λ_c candidates.

Since the initial collision center of mass energy is set to match the $\Upsilon(4S)$ resonance, which decays into a $B\bar{B}$ pair, one can use the following two kinematic variables to identify the reconstructed B meson candidates: the beam constrained mass $M_{\rm bc} = \sqrt{E_{\rm beam}^2 - p_B^2}$, and the energy difference $\Delta E = E_B - E_{\rm beam}$, where $E_{\rm beam}$, p_B, and E_B are the beam energy, the momentum, and energy of the reconstructed B meson, respectively, in the rest frame of the $\Upsilon(4S)$. The candidate region is defined as $5.2 < M_{\rm bc} < 5.29$ GeV/c^2 and $|\Delta E| < 0.2$ GeV.

The dominant background arises from the continuum $e^+e^- \to q\bar{q}$ process, with much smaller contributions from "cross feed," where similar types of rare decay events pass each other's signal criteria. The background from charm-bearing and charmless mesonic decays is negligible. In the $\Upsilon(4S)$ rest frame, continuum events are jetlike, while $B\bar{B}$ events are more spherical. One can use the reconstructed momenta of final state particles to form various shape variables (e.g., thrust angle, Fox-Wolfram moments, etc.) in order to categorize each event. We follow the scheme defined in Ref. [15] that combines seven event shape variables into a Fisher discriminant [16] in order to suppress continuum background. The variables chosen have almost no correlation with $M_{\rm bc}$ and ΔE. Probability density functions (PDFs) for the Fisher discriminant and the cosine of the angle between the B flight direction and the beam direction in the $\Upsilon(4S)$ rest frame are combined to form the signal (background) likelihood $\mathcal{L}_{s(b)}$. The signal PDFs are determined using signal MC simulation; the background PDFs are obtained from the continuum MC simulation for events with $5.27 < M_{\rm bc} < 5.29$ GeV/c^2 and $|\Delta E| < 0.1$ GeV. We require the likelihood ratio $\mathcal{LR} = \mathcal{L}_s/(\mathcal{L}_s + \mathcal{L}_b)$ to be greater than 0.8, 0.9, 0.85, 0.8, and 0.8 for $p\bar{p}K^+$, $p\bar{p}\pi^+$, $p\bar{p}K_S^0$, $p\bar{p}K^{*+}$, and $p\bar{p}K^{*0}$ modes, respectively. The selection points are determined by optimization of $N_s/\sqrt{(N_s + N_b)}$, where N_s and N_b denote the number of signal and background, respectively. Note that a nominal signal branching fraction of 4×10^{-6} is assumed.

Since the previous studies [1,2] showed an enhancement at low baryon-antibaryon invariant mass, we first focus on the near threshold region by requiring $M_{p\bar{p}} < 2.85$ GeV/c^2 to make sure it is below charmonium threshold. The $M_{\rm bc}$ distributions (with $|\Delta E| < 0.05$ GeV) and the ΔE distributions (with $M_{\rm bc} > 5.27$ GeV/c^2) for the $p\bar{p}K^+$, $p\bar{p}\pi^+$, $p\bar{p}K_S^0$, and $p\bar{p}K^{*+}$ modes are shown in Fig. 1. We use an unbinned likelihood fit to estimate the signal yield:

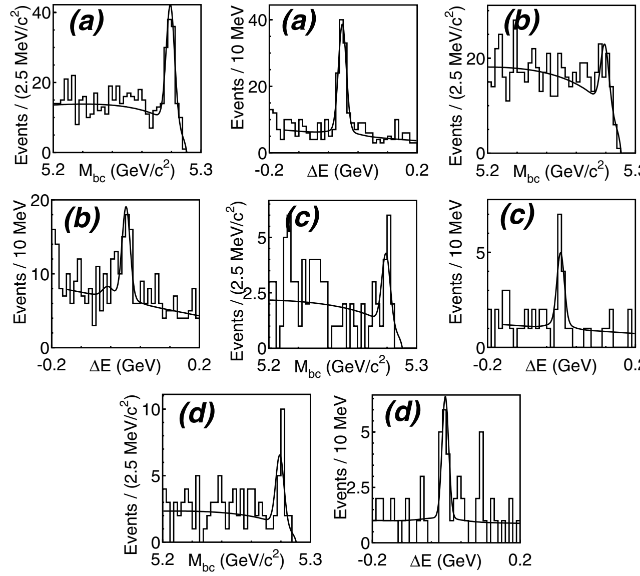

FIG. 1. $M_{\rm bc}$ and ΔE distributions for (a) $p\bar{p}K^+$, (b) $p\bar{p}\pi^+$, (c) $p\bar{p}K_S^0$, and (d) $p\bar{p}K^{*+}$ modes, for $M_{p\bar{p}} < 2.85$ GeV/c^2.

$$L = \prod_{i=1}^{N}[f_s P_s(M_{{\rm bc}_i}, \Delta E_i) + (1 - f_s)P_b(M_{{\rm bc}_i}, \Delta E_i)],$$

where P_s (P_b) denotes the signal (background) PDF and f_s is the signal fraction of the total N candidates. For the signal PDF, we use a Gaussian in $M_{\rm bc}$ and a double Gaussian in ΔE. We fix the parameters of these functions to values determined by MC simulation. Background shapes are studied using sideband events: $0.1 < |\Delta E| < 0.2$ GeV for the $M_{\rm bc}$ study and $5.20 < M_{\rm bc} < 5.26$ GeV/c^2 for ΔE. These shapes are confirmed with a continuum MC sample. We use the following parametrization first used by the ARGUS Collaboration, $f(M_{\rm bc}) \propto M_{\rm bc}\sqrt{1 - x^2}\exp[-\xi(1 - x^2)]$, to model the $M_{\rm bc}$ background, where x is defined as $M_{\rm bc}/E_{\rm beam}$ and ξ is a parameter to be fit. The ΔE background shape is modeled by a first order polynomial. There are possible cross feeds from $p\bar{p}K^{*+}$ and $p\bar{p}K^{*0}$ modes to $p\bar{p}K^+$, $p\bar{p}\pi^+$, and $p\bar{p}K_S^0$ modes; therefore, the cross-feed region ($\Delta E < -0.16$ GeV) is excluded in the fit. Since the $p\bar{p}\pi^+$ mode can contain non-negligible cross-feed events from the $p\bar{p}K^+$ mode, we include the $p\bar{p}K^+$ MC cross-feed shape in the fit for the determination of the $p\bar{p}\pi^+$ yield. The fit results are shown in Fig. 1 by solid curves. The fit yields are $96.4^{+11.2}_{-10.5}$, $37.4^{+8.1}_{-7.7}$, $11.3^{+4.1}_{-3.4}$, and $14.5^{+4.6}_{-4.0}$ with significances of 15.3, 6.7, 5.1, and 6.0 standard deviations for the $p\bar{p}K^+$, $p\bar{p}\pi^+$, $p\bar{p}K_S^0$, and $p\bar{p}K^{*+}$ modes, respectively. The significance is defined as $\sqrt{-2\ln(L_0/L_{\rm max})}$ [17], where L_0 and $L_{\rm max}$ denote the likelihood with signal yield fixed at zero and at the fitted value, respectively.

Although we do not have adequate statistics to perform a full Dalitz plot analysis, the observed distribution is not uniform over phase space. To reduce the model dependence in determining the branching fraction, we fit the signal yields separately in nine bins of $M_{p\bar{p}}$ and correct for the detection efficiencies from MC simulation in each bin. In Fig. 2, we show the signal yield versus $M_{p\bar{p}}$, with three-body phase space from MC (normalized in area) superimposed. The observed mass distributions all peak at low $p\bar{p}$ mass. The branching fractions ($\mathcal{B}$) in bins of $M_{p\bar{p}}$ for the observed modes are given in Table I. The upper limit of the last bin is different for each mode and is equal to the kinematic limit, $M_{p\bar{p}-\mathrm{lim}}$. We sum the partial branching fractions to obtain the total branching fractions. The results are listed in Table II and the branching fractions below charmonium threshold, $M_{p\bar{p}} < 2.85$ GeV/c^2, are also listed for comparison. Note that $\mathcal{B}(B^0 \to p\bar{p}K^0) = 2\mathcal{B}(B^0 \to p\bar{p}K_S^0)$ is assumed.

The search for $p\bar{p}K^{*0}$ gives a yield of 13^{+6}_{-5} events with a significance of about 3 standard deviations. Since it is less significant, we use the fit results to estimate the expected background and compare this with the observed number of events in the signal region in order to set the upper limit on the yield at the 90% confidence level [18,19]. Note that the systematic uncertainty is needed in this estimation. The upper limit yield of the $p\bar{p}K^{*0}$ mode in the full $M_{p\bar{p}}$ range is determined to be 57 at the 90% confidence level. The branching fraction is found to be $\mathcal{B}(B^0 \to p\bar{p}K^{*0}) < 7.6 \times 10^{-6}$.

Systematic uncertainties are studied using high statistics control samples. For proton identification, we use a $\Lambda \to p\pi^-$ sample, while for K/π identification we use a $D^{*+} \to D^0\pi^+$, $D^0 \to K^-\pi^+$ sample. Tracking efficiency is studied with fully and partially reconstructed D^* samples. K_S^0 reconstruction efficiency is studied with a $D^- \to K_S^0\pi^-$ sample. The $\mathcal{LR}$ continuum suppression uncertainty is studied with $B^+ \to J/\psi K^+$, $B^0 \to J/\psi K_S^0$, $B^+ \to J/\psi K^{*+}$, and $B^0 \to J/\psi K^{*0}$ (with $J/\psi \to \mu^+\mu^-$) control samples. Based on these studies, we assign a 1% error for each track, 3% for each proton identification, 2% for each kaon/pion identification, 5% for K_S^0 reconstruction, and 6% for the $\mathcal{LR}$ selection.

The systematic uncertainty in the fit yield is studied by varying the parameters of the signal and background PDFs. We assign an error of 5% for the $p\bar{p}\pi^+$ mode and 4% for the other modes. There is a possibility of nonresonant $K_S^0\pi^+$ combinations passing our K^{*+} cut. We

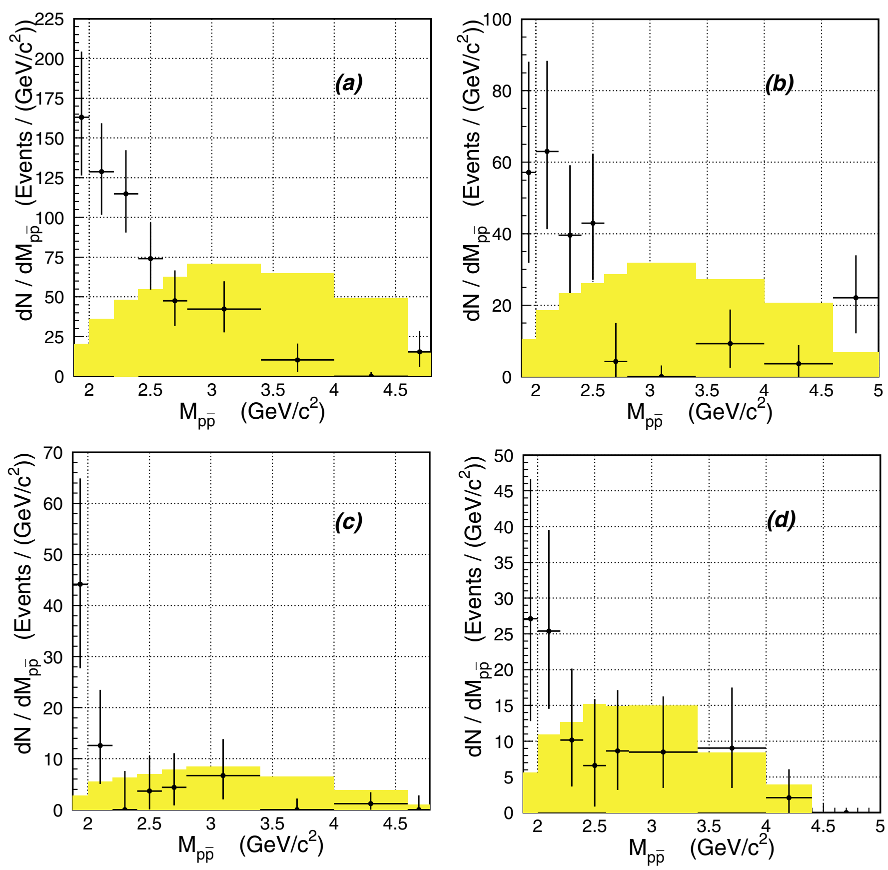

FIG. 2 (color online). Fitted signal yield divided by the bin size for (a) $p\bar{p}K^+$, (b) $p\bar{p}\pi^+$, (c) $p\bar{p}K_S^0$, and (d) $p\bar{p}K^{*+}$ modes in bins of $M_{p\bar{p}}$. The shaded distribution is from the phase-space MC simulation with area normalized to signal yield.

TABLE I. Branching fractions (in units of 10^{-6}) in different $M_{p\bar{p}}$ bins for the $p\bar{p}K^+$, $p\bar{p}\pi^+$, $p\bar{p}K_S^0$, and $p\bar{p}K^{*+}$ modes.

$M_{p\bar{p}}$ (GeV/c^2)	$p\bar{p}K^+$	$p\bar{p}\pi^+$	$p\bar{p}K_S^0$	$p\bar{p}K^{*+}$
$1.876-2.0$	$0.91^{+0.23}_{-0.20}$	$0.29^{+0.15}_{-0.13}$	$0.38^{+0.18}_{-0.14}$	$1.40^{+1.01}_{-0.74}$
$2.0-2.2$	$1.33^{+0.31}_{-0.28}$	$0.57^{+0.23}_{-0.20}$	$0.17^{+0.15}_{-0.10}$	$2.11^{+1.17}_{-0.90}$
$2.2-2.4$	$1.20^{+0.29}_{-0.25}$	$0.39^{+0.19}_{-0.16}$	$0.00^{+0.12}_{-0.12}$	$1.01^{+1.00}_{-0.65}$
$2.4-2.6$	$0.82^{+0.25}_{-0.22}$	$0.46^{+0.21}_{-0.17}$	$0.06^{+0.12}_{-0.06}$	$0.64^{+0.91}_{-0.56}$
$2.6-2.8$	$0.51^{+0.21}_{-0.17}$	$0.05^{+0.12}_{-0.12}$	$0.08^{+0.12}_{-0.06}$	$0.95^{+0.94}_{-0.60}$
$2.8-3.4$	$0.53^{+0.22}_{-0.18}$	$0.00^{+0.04}_{-0.04}$	$0.14^{+0.15}_{-0.10}$	$1.19^{+1.09}_{-0.71}$
$3.4-4.0$	$0.15^{+0.15}_{-0.11}$	$0.15^{+0.16}_{-0.11}$	$0.00^{+0.07}_{-0.07}$	$2.07^{+1.93}_{-1.28}$
$4.0-4.6$	$0.00^{+0.08}_{-0.08}$	$0.15^{+0.21}_{-0.21}$	$0.10^{+0.19}_{-0.10}$	$0.93^{+1.75}_{-1.75}$
$4.6-M_{p\bar{p}-\text{lim}}$	$0.20^{+0.17}_{-0.12}$	$1.00^{+0.54}_{-0.45}$	$0.00^{+0.11}_{-0.11}$	

study this by fitting for the B yield in bins of $M_{K_S^0\pi^+}$. Choosing a Breit-Wigner signal and a first order polynomial background to estimate the $B^+ \to p\bar{p}K^{*+}$ branching fraction, the number drops by 9%. We include this uncertainty in the estimation of signal yield for the $p\bar{p}K^{*+}$ mode. The MC statistical uncertainty and modeling with nine $M_{p\bar{p}}$ bins contributes a 2% error in the branching fraction determination. The error on the number of $B\bar{B}$ pairs is determined to be 1%, where an assumption is made that the branching fractions of $\Upsilon(4S)$ to neutral and charged $B\bar{B}$ pairs are equal.

We first sum the correlated errors linearly (e.g., total 5% tracking error for the $p\bar{p}K^{*+}$ mode) and then combine with the uncorrelated ones in quadrature. The determined systematic uncertainties are 11%, 12%, 12%, $^{+13}_{-16}$%, and 13% for the $p\bar{p}K^+$, $p\bar{p}\pi^+$, $p\bar{p}K^0$, $p\bar{p}K^{*+}$, and $p\bar{p}K^{*0}$ modes, respectively.

Using the charm veto events, we perform a cross-check of our analysis. We determine $B \to J/\psi K^{(*)}$ branching fractions by following the same analysis procedure with $3.07 < M_{p\bar{p}} < 3.11$ GeV/c^2 and using $\mathcal{B}(J/\psi \to p\bar{p}) = (2.12 \pm 0.10 \times 10^{-3})$ [17]. The obtained branching fractions are $\mathcal{B}(B^+ \to J/\psi K^+) = (1.17^{+0.12}_{-0.13} \pm 0.16) \times 10^{-3}$, $\mathcal{B}(B^0 \to J/\psi K^0) = (1.16^{+0.24}_{-0.24} \pm 0.16) \times 10^{-3}$, $\mathcal{B}(B^+ \to J/\psi K^{*+}) = (1.08^{+0.51}_{-0.42} \pm 0.17) \times 10^{-3}$, and $\mathcal{B}(B^0 \to J/\psi K^{*0}) = (1.40^{+0.27}_{-0.26} \pm 0.21) \times 10^{-3}$, which are in agreement with the world average values [17].

The present results, shown in Table II, offer valuable information for understanding the mechanism of charmless baryonic B decay. In particular, the threshold peaking behavior is now firmly established. The $B^+ \to p\bar{p}K^+$ data can be used to constrain the production of narrow glueball states that decay to $p\bar{p}$ [7]. With the current statistics, we cannot set a very stringent bound. It should be noted that the observed $B^+ \to p\bar{p}\pi^+$ rate is less than $B^+ \to p\bar{p}K^+$, which is consistent with what is observed in $B \to K\pi$, $\pi\pi$ modes. The $B^0 \to p\bar{p}K^0$ rate is considerably lower than that of the $B^+ \to p\bar{p}K^+$ mode which should be contrasted with $B^{0,+} \to \pi^0 K^{0,+}$ modes and also $B^{0,+} \to J/\psi K^{0,+}$ modes. This indicates that the intermediate $p\bar{p}$ system is nontrivial. These modes are of

TABLE II. Branching fractions (in units of 10^{-6}) in the full $M_{p\bar{p}}$ range and below the charm threshold ($M_{p\bar{p}} <$ 2.85 GeV/c^2) for the $p\bar{p}K^+$, $p\bar{p}\pi^+$, $p\bar{p}K_S^0$, and $p\bar{p}K^{*+}$ modes. Statistical and systematic errors are quoted.

Mode	Full $M_{p\bar{p}}$ range	$M_{p\bar{p}} < 2.85$ GeV/c^2
$B^+ \to p\bar{p}K^+$	$5.66^{+0.67}_{-0.57} \pm 0.62$	$4.89^{+0.59}_{-0.55} \pm 0.54$
$B^+ \to p\bar{p}\pi^+$	$3.06^{+0.73}_{-0.62} \pm 0.37$	$1.76^{+0.42}_{-0.37} \pm 0.21$
$B^0 \to p\bar{p}K^0$	$1.88^{+0.77}_{-0.60} \pm 0.23$	$1.56^{+0.52}_{-0.49} \pm 0.19$
$B^+ \to p\bar{p}K^{*+}$	$10.3^{+3.6+1.3}_{-2.8-1.7}$	$6.7^{+2.4+0.9}_{-2.0-1.1}$

interest for direct CP violation searches. For the $B^\mp \to p\bar{p}K^\mp$ and $p\bar{p}\pi^\mp$ modes that have larger statistics, we define the charge asymmetry as $(N_{B^-} - N_{B^+})/(N_{B^-} + N_{B^+})$ and find the values are $-0.05 \pm 0.11 \pm 0.01$ and $-0.16 \pm 0.22 \pm 0.01$, respectively. The systematic error is determined by checking the null asymmetry with a $B \to D(\to K\pi)\pi$ control sample. The measured asymmetries are consistent with zero for their large statistical uncertainties.

We wish to thank the KEKB accelerator group for the excellent operation of the KEKB accelerator. We acknowledge support from the Ministry of Education, Culture, Sports, Science, and Technology of Japan and the Japan Society for the Promotion of Science; from the Australian Research Council and the Australian Department of Education, Science and Training; from the National Science Foundation of China under Contract No. 10175071; from the Department of Science and Technology of India; from the BK21 program of the Ministry of Education of Korea and the CHEP SRC program of the Korea Science and Engineering Foundation; from the Polish State Committee for Scientific Research under Contract No. 2P03B 01324; from the Ministry of Science and Technology of the Russian Federation; from the Ministry of Education, Science and Sport of the Republic of Slovenia; from the National Science Council and the Ministry of Education of Taiwan; and from the U.S. Department of Energy.

*On leave from Nova Gorica Polytechnic, Nova Gorica.

[1] Belle Collaboration, K. Abe *et al.*, Phys. Rev. Lett. **88**, 181803 (2002).
[2] Belle Collaboration, M. Z. Wang *et al.*, Phys. Rev. Lett. **90**, 201802 (2003).
[3] H. Y. Cheng and K. C. Yang, Phys. Rev. D **66**, 014020 (2002).
[4] C. K. Chua, W. S. Hou, and S. Y. Tsai, Phys. Rev. D **66**, 054004 (2002).
[5] M. Suzuki, J. Phys. G **29**, B15 (2003).
[6] C. K. Chua and W. S. Hou, Eur. Phys. J. C **29**, 27 (2003).
[7] C. K. Chua, W. S. Hou, and S. Y. Tsai, Phys. Lett. B **544**, 139 (2002).

[8] B. Kirbikov, A. Stavinsky, and V. Fedotov, nucl-th/0310060.
[9] J. L. Rosner, Phys. Rev. D **68**, 014004 (2003).
[10] W. S. Hou and A. Soni, Phys. Rev. Lett. **86**, 4247 (2001).
[11] C. K. Chua, W. S. Hou, and S. Y. Tsai, Phys. Lett. B **528**, 233 (2002).
[12] Throughout this report, inclusion of charge conjugate mode is always implied unless otherwise stated.
[13] S. Kurokawa *et al.*, Nucl. Instrum. Methods Phys. Res., Sect. A **499**, 1 (2003).
[14] Belle Collaboration, A. Abashian *et al.*, Nucl. Instrum. Methods Phys. Res., Sect. A **479**, 117 (2002).
[15] Belle Collaboration, K. Abe *et al.*, Phys. Lett. B **517**, 309 (2001).
[16] R. A. Fisher, Ann. Eugenics **7**, 179 (1936).
[17] Particle Data Group, K. Hagiwara *et al.*, Phys. Rev. D **66**, 010001 (2002).
[18] G. J. Feldman and R. D. Cousins, Phys. Rev. D **57**, 3873 (1998).
[19] J. Conrad *et al.*, Phys. Rev. D **67**, 012002 (2003).